

## MIT Open Access Articles

*Role of phonon dispersion in studying  
phonon mean free paths in skutterudites*

The MIT Faculty has made this article openly available. **Please share** how this access benefits you. Your story matters.

**Citation:** Zebarjadi, Mona et al. "Role of Phonon Dispersion in Studying Phonon Mean Free Paths in Skutterudites." *Journal of Applied Physics* 112.4 (2012): 044305. CrossRef. Web. © 2012 American Institute of Physics.

**As Published:** <http://dx.doi.org/10.1063/1.4747911>

**Publisher:** American Institute of Physics

**Persistent URL:** <http://hdl.handle.net/1721.1/78284>

**Version:** Final published version: final published article, as it appeared in a journal, conference proceedings, or other formally published context

**Terms of Use:** Article is made available in accordance with the publisher's policy and may be subject to US copyright law. Please refer to the publisher's site for terms of use.



## Role of phonon dispersion in studying phonon mean free paths in skutterudites

Mona Zebarjadi, Jian Yang, Kevin Lukas, Boris Kozinsky, Bo Yu et al.

Citation: *J. Appl. Phys.* **112**, 044305 (2012); doi: 10.1063/1.4747911

View online: <http://dx.doi.org/10.1063/1.4747911>

View Table of Contents: <http://jap.aip.org/resource/1/JAPIAU/v112/i4>

Published by the [American Institute of Physics](#).

---

### Additional information on J. Appl. Phys.

Journal Homepage: <http://jap.aip.org/>

Journal Information: [http://jap.aip.org/about/about\\_the\\_journal](http://jap.aip.org/about/about_the_journal)

Top downloads: [http://jap.aip.org/features/most\\_downloaded](http://jap.aip.org/features/most_downloaded)

Information for Authors: <http://jap.aip.org/authors>

## ADVERTISEMENT



**AIPAdvances**

Now Indexed in Thomson Reuters Databases

Explore AIP's open access journal:

- Rapid publication
- Article-level metrics
- Post-publication rating and commenting

## Role of phonon dispersion in studying phonon mean free paths in skutterudites

Mona Zebarjadi,<sup>1</sup> Jian Yang,<sup>2</sup> Kevin Lukas,<sup>2</sup> Boris Kozinsky,<sup>3</sup> Bo Yu,<sup>2</sup> Mildred S. Dresselhaus,<sup>4</sup> Cyril Opeil,<sup>2</sup> Zhifeng Ren,<sup>2</sup> and Gang Chen<sup>1</sup>

<sup>1</sup>*Department of Mechanical Engineering, Massachusetts Institute of Technology, Cambridge, Massachusetts 02139, USA*

<sup>2</sup>*Department of Physics, Boston College, Chestnut Hill, Massachusetts 02467, USA*

<sup>3</sup>*Research and Technology Center, Robert Bosch LLC, Cambridge, Massachusetts 02142, USA*

<sup>4</sup>*Department of Physics and Department of Electrical Engineering and Computer Science, Massachusetts Institute of Technology, Cambridge, Massachusetts 02139, USA*

(Received 24 April 2012; accepted 20 July 2012; published online 23 August 2012)

Experimental thermal conductivity of bulk materials are often modeled using Debye approximation together with functional forms of relaxation time with fitting parameters. While such models can fit the temperature dependence of thermal conductivity of bulk materials, the Debye approximation leads to large error in the actual phonon mean free path, and consequently, the predictions of the thermal conductivity of the nanostructured materials using the same relaxation time are not correct even after considering additional size effect on the mean free path. We investigate phonon mean free path distribution inside fully unfilled (Co<sub>4</sub>Sb<sub>12</sub>) and fully filled (LaFe<sub>4</sub>Sb<sub>12</sub>) bulk skutterudites by fitting their thermal conductivity to analytical models which employ different phonon dispersions. We show that theoretical thermal conductivity predictions of the nanostructured samples are in agreement with the experimental data obtained for samples of different grain sizes only when the full phonon dispersion is considered. © 2012 American Institute of Physics. [<http://dx.doi.org/10.1063/1.4747911>]

### INTRODUCTION

Thermoelectric power generators can directly convert heat into electricity. The efficiency of a thermoelectric device is an increasing function of the material's figure-of-merit,  $ZT = \sigma S^2 T / \kappa$ , where  $\sigma$  is the electrical conductivity,  $S$  is the Seebeck coefficient;  $T$  is the absolute temperature, and  $\kappa$  is the thermal conductivity. A successful strategy in enhancing  $ZT$  is through reducing the phonon thermal conductivity by alloying,<sup>1</sup> nanostructuring,<sup>2</sup> or introducing rattling atoms into materials with cage-like structures, such as skutterudites.<sup>3</sup> In all these cases, it has been shown that phonons could be scattered more significantly than electrons, leading to a higher  $\sigma/\kappa$  ratio. While alloying affects low wavelength phonons of less than 1 nm, nanostructuring involves larger scales and can scatter mid to long wavelength phonons. Rattling atoms only scatter phonons which have frequencies close to those of the rattler's vibrations. To predict how nanostructuring affects the thermal conductivity, the knowledge of bulk phonon wavelengths and their mean free paths is required. Grain boundary interfaces can scatter phonons with mean free paths larger than the grain interface spacing, but they will not affect phonons with mean free paths much shorter than the interfacial separation distances. To find the phonon mean free path spectrum in a specific bulk material, it is very common to fit the thermal conductivity versus temperature by adjusting several parameters and then to back calculate the phonon mean free path spectrum. The thermal conductivity can be calculated knowing the dispersion relations and relaxation times for the relevant scattering processes. Phonon dispersion relations can be obtained

accurately from first-principles calculations without involving much computation. The relaxation times are difficult to extract from first-principles calculations.<sup>4</sup> Recently there have been several valuable attempts to extract phonon-phonon scattering from first-principles,<sup>5-9</sup> but such computations are still time consuming and difficult to perform for each new material. Moreover, in practice, phonon-phonon scattering is not the only important scattering mechanism for nanocomposite thermoelectric materials. Often, there is a significant contribution to the total phonon scattering cross section from electrons, point defects, impurities, dangling bonds, random inhomogeneities, and boundary scatterings. For these scattering processes, only phenomenological models are applicable so far. Another difficulty is that there is a large uncertainty regarding the experimental density of the defects and what the grain boundaries look like. Therefore, fitting seems to be a reasonable approach for these cases.

The lattice thermal conductivity of bulk single crystals versus temperature ( $\kappa_L(T)$ ) usually has a standard behavior. It starts from zero at zero temperature, increases to a peak value versus temperature, and then drops at high temperatures. This trend can be easily fitted using simple models and the simplest band dispersions such as the Debye dispersion. Three fitting parameters are often enough to get a perfect fit. Low temperature behavior can be fitted by adjusting the size scale of the sample boundaries, the middle range by the impurity density, and the high temperature range through adjusting the phonon-phonon coupling. However, depending on the dispersion used, different fitting parameters and different predicted phonon mean free path spectra could be

obtained which then impose uncertainty on the design of the nanostructured materials.

Chen<sup>10</sup> compared several models to predict the lattice thermal conductivity of GaAs/AlAs superlattices. He proposed three models: the gray medium (constant mean free path model) without dispersion which is the simplest but least accurate model; the gray medium with dispersion (sine dispersion), and the non-gray medium with dispersion which is the most accurate one and its predictions are in agreement with the experimental data. They showed that both sine dispersion and model of Holland can fit the thermal conductivity of bulk GaAs with different sets of fitting parameters.<sup>11</sup>

Chung *et al.*<sup>12</sup> discussed the importance of the phonon dispersion in fitting the thermal conductivity data of germanium using the Holland model.<sup>13</sup> They observed a non-physical discontinuity in the transverse phonon relaxation times. However, they did not extend their analysis to find the differences in the phonon mean free paths. Baillis and Randraianalisoa<sup>14</sup> studied the effect of phonon dispersion to predict the in-plane and the out-of-plane thermal conductivity of silicon thin films and nanowires. They used the Holland dispersion and the Brillouin zone boundary condition dispersion models to fit the experimental data of bulk silicon and to predict the thermal conductivity of silicon nanostructures. They concluded that there is a significant discrepancy between the predictions of the two models, and that the Holland model overestimates the thermal conductivity of the nanostructures. A similar conclusion was also reached by Mingo<sup>15</sup> when comparing full phonon dispersion results with those of the Callaway model.<sup>16</sup>

In this paper, we compare the Debye dispersion results with those of the full phonon dispersion obtained from first-principles calculations and apply them specifically to the case of skutterudites. First, we show that there is a clear difference in the calculated phonon mean free path spectrum using the two different dispersion relations. Second, through a systematic experimental study, we quantify the effect of grain size on the lattice thermal conductivities. The experimental data will be compared to the theoretical predictions. Although both dispersion relations can lead to a good fit to the thermal conductivity of large grained bulk skutterudites, we show that it is only when considering the full dispersion (FD) that correct results are obtained in the predictions of the thermal conductivity of nanostructured unfilled skutterudites ( $\text{Co}_4\text{Sb}_{12}$ ) and fully filled skutterudites ( $\text{LaFe}_4\text{Sb}_{12}$ ).

The paper is organized as follows. First, we describe the experimental procedure of making and characterizing samples with different grain sizes. Then, we describe the modeling and apply it to pure skutterudites as well as to fully filled skutterudites. We fit the thermal conductivity of bulk  $\text{Co}_4\text{Sb}_{12}$  and  $\text{LaFe}_4\text{Sb}_{12}$  versus temperature using two different dispersions: a full dispersion obtained from first principles and a Debye dispersion. The phonon mean free path spectrum is then extracted from each model. Based on the obtained phonon mean free path spectrum, we predict the lattice thermal conductivity of the nanocomposites of different grain sizes and finally we compare the predictions with those of the experiments.

## EXPERIMENT

The polycrystalline  $\text{Co}_4\text{Sb}_{12}$  and  $\text{LaFe}_4\text{Sb}_{12}$  samples were made by following the method from Ref. 17. Polycrystalline samples were synthesized by melting stoichiometric amounts of high purity constituents in sealed carbon coated quartz tubes. The tubes were then loaded into a box furnace and heated to 600 °C at 1 °C/min and then to 1080 °C at 2 °C/min. After soaking at 1080 °C for 20 h, the quartz tubes containing the homogeneous molten liquid were then quenched in a water bath, followed by an annealing of 30 h at 700 °C. The as-prepared solids were then taken out from the tubes and cleaned with a wire brush before an additional ball milling process in high-energy ball mills with stainless grinding vial sets. The as-milled powders were finally consolidated into bulk pellets in a graphite die by a direct current-hot press method. Bar and disc-shaped samples were cut from those pellets for the characterization of the thermoelectric transport properties (bar shape for ZEM and PPMS setups and disk shape for the laser flash setup). The grain sizes were controlled by means of changing the ball milling time (from a few minutes to more than 10 h) and the pressing temperature (800–1000 K). We used a commercial four-probe system (ZEM-3, ULVAC-RIKO) to measure the electrical conductivity and a laser flash system (LFA 457, Netzsch), for thermal conductivity measurements, from 300 K to 700 K. A physical properties measurement system (PPMS) from Quantum Design was used for low temperature characterizations. The lattice thermal conductivity contribution was extracted using the Wiedemann–Franz law and a constant Lorenz number of  $2.4 \times 10^{-8} \text{ W } \Omega \text{ K}^{-2}$ . Here, we assume that the contribution from bipolar effects is small in the temperature region that we are studying.

## RESULTS AND DISCUSSION

### Pure skutterudites ( $\text{Co}_4\text{Sb}_{12}$ )

In what follows, we explain our methodology for extracting the thermal conductivity from the full dispersion and Debye models. First principles based phonon dispersion calculations of  $\text{Co}_4\text{Sb}_{12}$  have been reported before in several published works.<sup>18,19</sup> Our dispersion (see Fig. 1) is in agreement with those of Feldman and Singh<sup>18</sup> and was reported elsewhere.<sup>20</sup> We obtain phonon frequencies ( $\omega$ ) for each  $q$  point in the first Brillouin zone and for each mode ( $\lambda$ ). Having phonon dispersions, the group velocities ( $\partial\omega_\lambda/\partial\vec{q}$ ) can be calculated for each mode and at each  $q$  point in reciprocal space. The skutterudite crystal structure has a cubic symmetry, and therefore has isotropic thermal conductivities. The thermal conductivity for an isotropic structure can be written as

$$k = \frac{1}{3n_q\Omega} \sum_\lambda \sum_{q \in \text{FBZ}} \hbar\omega_\lambda(\vec{q})v_\lambda^2(\vec{q})\tau_\lambda(\vec{q}) \frac{\partial n}{\partial T} \quad (1)$$

where  $\vec{q}$  is the wave vector,  $\lambda$  is the mode index (branch index),  $v_\lambda$  is the group velocity for the  $\lambda$  mode,  $n$  is the Bose-Einstein distribution function,  $n_q$  is the number of  $q$  points sampling the first Brillouin zone,  $\Omega$  denotes the primitive

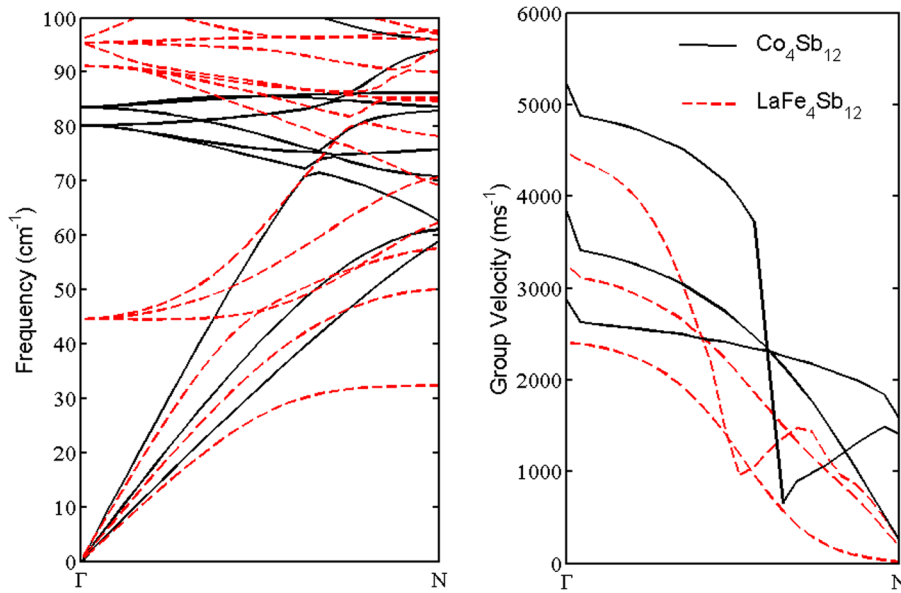


FIG. 1. Phonon dispersion (left) and group velocity amplitudes (right) along the  $\Gamma N$  [110] direction, calculated from first principles on a  $50 \times 50 \times 50$  mesh. In the thermal conductivity calculations, we only included first 6 bands of each material. For clarity purposes, we only plotted the group velocities for the acoustic bands.

cell volume, and  $\tau$  is the relaxation time. The dispersion and the group velocities along the  $\Gamma N$  [110] direction in the Brillouin Zone are shown in Fig. 1.

For the Debye formalism, we follow the modeling of Ref. 28. Equation (1) could be simplified by using the Debye dispersion. In this model, the group velocity is a constant number and is assumed to be independent of the modes and  $\vec{q}$  points, namely the sound velocity of the material ( $\omega = v_s q$ ). Converting the sum over the  $\vec{q}$  points into an integral over the frequencies, we obtain the following expression for the thermal conductivity within the Debye model:

$$k = \int_0^{\omega_D} d\omega g(\omega) \hbar \omega v_s^2 \tau(\omega) \frac{\partial n}{\partial T}, \quad (2)$$

$$\int_0^{\omega_D} d\omega g(\omega) = 3N, \quad (3)$$

where  $\omega_D$  is the Debye frequency ( $\hbar \omega_D = k_B \theta_D$ ),  $v_s$  is the sound velocity, and  $\theta_D$  is the Debye temperature. For  $\text{Co}_4\text{Sb}_{12}$ ,  $\theta_D = 307$  K and  $v_s = 2.93 \times 10^5$  cm/s. These values are obtained from experimental measurements.<sup>28</sup> Following Ref. 28, three scattering mechanisms are included to calculate the frequency dependent relaxation times including phonon-phonon scattering ( $\tau_{ph}$ ),<sup>21</sup> boundary scattering ( $\tau_{BC}$ ), and isotope or mass fluctuation scattering ( $\tau_{iso}$ )<sup>22</sup>

$$\tau^{-1} = \tau_{BC}^{-1} + \tau_{iso}^{-1} + \tau_{ph}^{-1} = \frac{v}{l_g} + Ax^4 T^4 + Bx^2 T^3 \exp\left(-\frac{\theta_D}{2T}\right);$$

$$x = \frac{\hbar \omega}{k_B T}, \quad (4)$$

where  $l_g$  is the average grain size,  $k_B$  is the Boltzmann constant, and A and B are fitting parameters representing the isotope scattering strength and the phonon-phonon coupling, respectively.

We use the same relaxation time model (Eq. (4)) and fit the experimental data of a sample with large grain size

(representing a bulk sample) with the two dispersions described above. For the Debye model, we use the measured Debye temperature of 307 K, and for the full dispersion, we use the calculated Debye temperature based on first-principles calculations<sup>18</sup> (200 K). The average grain size ( $l_g$ ) for our bulk sample is about  $2 \mu\text{m}$ . Figure 2 shows the measured lattice thermal conductivity over a wide temperature range, measured for this sample, and our fits based on the two different dispersions. As indicated, both models can fit the experimental data. Note that above 600 K, we start to see a contribution from the bipolar effect as the thermal conductivity starts to increase with increasing the temperature. This effect is not considered in our model.

Table I summarizes the fitting parameter values used for each model. There are big differences in the obtained values

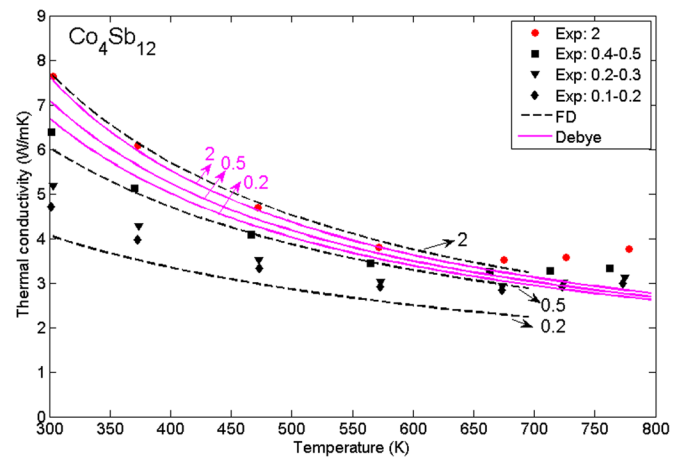


FIG. 2. Lattice thermal conductivity of  $\text{Co}_4\text{Sb}_{12}$  versus temperature: Experimental data are labeled as Exp., the numbers in front of Exp. indicates the range of grain sizes in microns. Solid lines are calculated based on the Debye model and dashed lines are calculated based on the full dispersion model. In each case, the highest curve is fitted to the experimental data of the sample with an average grain size of  $2 \mu\text{m}$  (red dots). The second curve is the model prediction for a sample with average grain size of  $0.5 \mu\text{m}$  and the lowest curve is the model prediction for a sample with average grain size of  $0.2 \mu\text{m}$ .

TABLE I. Fitting parameter values obtained from each model.

Sample	Method	# of fitting parameters	A ( $S^{-1} K^{-4}$ ) defect	B ( $S^{-1} K^{-3}$ ) Umklapp	D ( $10^{-15}s$ ) resonance	$\alpha$ ( $10^8 m^{-1}$ ) resonance	F ( $10^4 m^{-1} K^{-1}$ ) two-level tunneling	G ( $K^{-2}$ ) two-level tunneling	A0 ( $10^{32} S^{-3} K^{-2}$ ) resonance
Co <sub>4</sub> Sb <sub>12</sub>	Debye	2	116	99 500	0	0	0	0	0
Co <sub>4</sub> Sb <sub>12</sub>	Full dispersion	2	380	18 426	0	0	0	0	0
LaFe <sub>4</sub> Sb <sub>12</sub>	Ref. 31	6	440	17 000	7	30	20	2	0
LaFe <sub>4</sub> Sb <sub>12</sub>	Debye + Einstein	4	640	17 000	0	0	14	0	30.42
LaFe <sub>4</sub> Sb <sub>12</sub>	Full dispersion	3	6000	60 000	0	0	15.5	0	0

for the different fitting parameters. Especially the impurity density is much weaker while the phonon-phonon coupling is much stronger in the Debye model compared to the full dispersion model. Therefore, we expect to find a large discrepancy in terms of the mean free path spectrum.

Figure 3 shows the cumulative thermal conductivity versus phonon mean free path at room temperature and shows the prediction of the two models for the mean free path spectrum and the contribution of each mean free path to the total thermal conductivity.<sup>23</sup> According to the Debye model, almost all of phonons contributing to the thermal conductivity have mean free paths below 200 nm and therefore are not affected much by grain sizes greater than 200 nm. This roughly means that a sample with an average grain size of 200 nm should have a similar thermal conductivity as that of the bulk sample at room temperature. The full dispersion, in contrast, predicts that there is a large contribution to the total thermal conductivity from phonons with mean free paths larger than 200 nm, and predicts a maximum reduction of about 60% when the grain size is reduced to about 200 nm.

Figure 2 shows experimental data of the measured thermal conductivity for samples of different grain sizes of Co<sub>4</sub>Sb<sub>12</sub>. These samples were prepared as we explained in the experimental section (See Fig. 4 for SEM images). Figure 2 indicates a reduction of 40% (from 7.6 to 4.7 W m<sup>-1</sup> K<sup>-1</sup>) in the thermal conductivity at room temperature, when the average grain size decreases from a couple of microns down to about 100 to 200 nm. As explained above, this observation is only consistent with the full dispersion model. To further illustrate this, we have also included

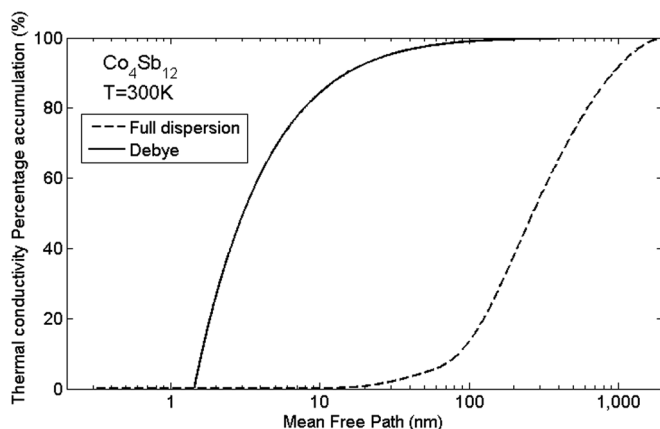


FIG. 3. Thermal conductivity percentage accumulation versus mean free path for Co<sub>4</sub>Sb<sub>12</sub> at room temperature calculated using two different dispersions: Debye dispersion and FD calculated from first principles.

in Fig. 2 the model predictions when the grain size is about 0.5  $\mu$ m and 0.2  $\mu$ m, respectively. Again the Debye model only shows a minor reduction, while the full dispersion model indicates a strong reduction in the thermal conductivity and is much closer to the experimental values. It should be noted that a direct comparison with the experiment is not possible since in the experiment there is a range of grain sizes and not a single size grains. We neither have a model to average over the different grain sizes nor do we have enough information on the exact experimental size distribution of the grains.

### Fully filled skutterudites (LaFe<sub>4</sub>Sb<sub>12</sub>)

In this section, we look at fully filled skutterudites. Unlike partially filled skutterudites which have randomness in their lattice structure, fully filled ones have periodic structures and therefore it is easier to investigate them theoretically.

Filled skutterudites are controversial in the literature. The rattling picture has been used widely for studying the thermal conductivity in these structures.<sup>24,25</sup> Based on this picture, skutterudites form relatively large cage-like structures. Filler atoms have weak bonds with the cage and therefore vibrate independently inside the host lattice. Large amplitude vibrations of the filler atoms in their cages have been confirmed experimentally,<sup>26,27</sup> but independent and incoherent vibrations have not. In terms of modeling, this means that in the presence of the filler atoms, one can approximate the phonon dispersion to be the same as that of the host matrix and only add flat optical bands to the dispersion to represent the filler atoms.<sup>28</sup> In a simplified model, known as the Debye + Einstein model, a Debye dispersion is taken for the phonon dispersion relation. Each optical band induced by the filler atoms is modeled only with a single frequency called the Einstein frequency. The phonons with frequencies close to the Einstein frequencies scatter largely from the filler atom vibrations (resonance scattering).<sup>29</sup> This phenomenological model has been quite successfully applied to different filled skutterudites where the experimental thermal conductivity data was fitted.<sup>24,28,30</sup>

We follow the same theoretical framework as we developed for pure skutterudites. The purpose is to look at the validity of the Debye + Einstein model for fully filled skutterudites. LaFe<sub>4</sub>Sb<sub>12</sub> has been chosen because there are available experimental data and already developed phenomenological models for this material in the literature.<sup>31</sup> We follow the studying of Ref. 31, in which a fully filled LaFe<sub>4</sub>Sb<sub>12</sub> bulk sample with large grain sizes (15  $\mu$ m on the

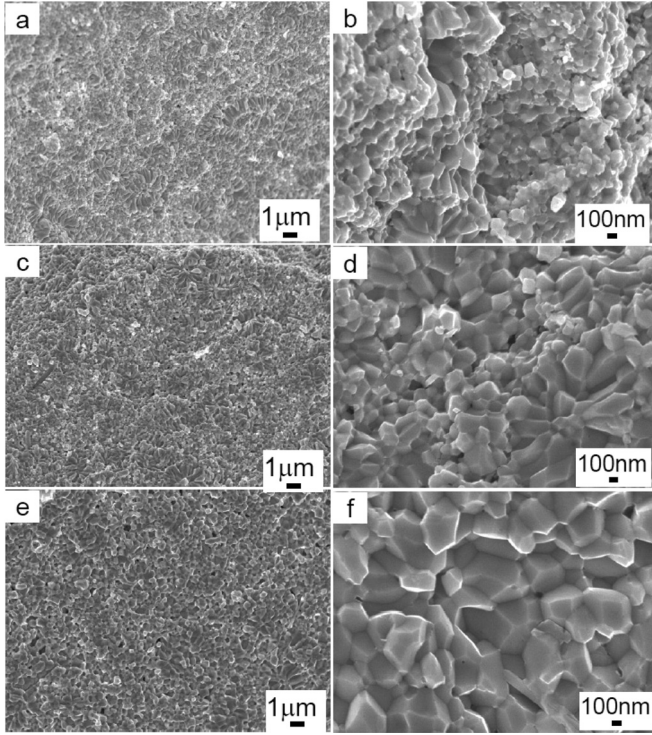


FIG. 4. Low- ((a), (c), and (e)) and high- ((b), (d), and (f)) magnification SEM images of the  $\text{Co}_4\text{Sb}_{12}$  samples with different grain sizes: 100–200 nm ((a) and (b)), 200–300 nm ((c) and (d)), 400–500 nm ((e) and (f)).

average) was made and characterized at low temperatures. These samples were analyzed and their measured thermal conductivity data were fitted by using a Debye + Einstein model.<sup>31</sup> Here we first explain the model developed in Ref. 31 and reproduce their results. Then like before, we use first-principles calculations to obtain the full phonon dispersion and fit for the relaxation times. We compare the results of the phonon mean free path distribution with the two different approaches. Finally, we compare the predictions of the two models with the experimental data for samples of different grain sizes.

In Ref. 31, to explain the experimental data for the fully filled  $\text{LaFe}_4\text{Sb}_{12}$ , a Debye based model has been developed. The model is similar to what we explained in the previous section for pure skutterudites. However, two scattering rates are introduced in addition to those introduced in Eq. (4), two-level tunneling ( $\tau_{TS}$ ) which is not the focus here and the resonance scattering ( $\tau_{RS}$ ). Resonance scattering is introduced to take care of the Einstein frequencies introduced in the phonon dispersion as a result of introduced filler atoms

$$\tau^{-1} = \tau_{BC}^{-1} + \tau_{iso}^{-1} + \tau_{ph}^{-1} + \tau_{TS}^{-1} + \tau_{RS}^{-1}, \quad (5)$$

$$\tau_{TS}^{-1} = v \left[ FTx \tanh\left(\frac{x}{2}\right) + \frac{1}{2}F \left( \frac{1}{Tx} + \frac{1}{GT^3} \right)^{-1} \right], \quad (6)$$

$$\tau_{RS}^{-1} = Df(\omega, T)g(\omega), \quad (7)$$

$$f(\omega, T) = \frac{(\omega_s - \omega)^2 e^{\frac{\hbar(\omega_s - \omega)}{k_B T}} \left( e^{\frac{\hbar\omega}{k_B T}} - 1 \right)}{\left( e^{\frac{\hbar\omega_k}{k_B T}} - 1 \right) \left( e^{\frac{\hbar(\omega_s - \omega)}{k_B T}} - 1 \right)},$$

$$g(\omega) = \left( 1 + 4 \frac{\alpha v}{\omega_s} \right) \ln \left[ \frac{\omega}{\alpha v} \left( 1 - \frac{\omega}{\omega_s} \right) + 1 \right] - 4 \frac{\omega}{\omega_s} \left( 1 - \frac{\omega}{\omega_s} \right),$$

$\omega_s$  is the Einstein frequency which can be related to the Einstein temperature  $\theta_s$ . For  $\text{LaFe}_4\text{Sb}_{12}$ ,  $\theta_D = 321$  K,  $\theta_s = 88$  K, and  $v_s = 3.078 \times 10^5$  cm/s which were measured experimentally.<sup>31</sup> The six parameters used to fit the data are  $A$  for defects,  $B$  for phonon-phonon coupling (see Eq. (4)),  $\alpha$  and  $D$  for resonance, and  $F$  and  $G$  for two-level tunneling. The values of these parameters are reported in Table I after Ref. 31. Reproduced theoretical data and experimental data of Ref. 31 are plotted in Figure 6. We also tried a more simplified model for resonance scattering which is usually used in the literature,<sup>28</sup> and has only one fitting parameter ( $A_0$ ) instead of two in the previous model ( $\alpha$  and  $D$ )

$$\tau_{RS}^{-1} = \frac{A_0 T^2 \omega^2}{(\omega^2 - \omega_s^2)^2}. \quad (8)$$

Also as an attempt to reduce the number of fitting parameters, we realized that the results are not sensitive to the  $G$  parameter. Therefore, for our second fitting, we took the  $G$  parameter out. In the figure legends and tables, we call this model Debye + Einstein model. But one should note that the Ref. 31 formalism is also a Debye + Einstein model and only uses a different expression for the resonance scattering. The results of our second fitting are reported in Table I and Fig. 5. Again we can fit the experimental data easily with this second Debye + Einstein model. Finally, we use the full dispersion model calculated from first principles and fit the relaxation times to obtain a third fit to the experimental data. This time, we do not include any resonance scattering term as it is unnecessary when the full band dispersion including

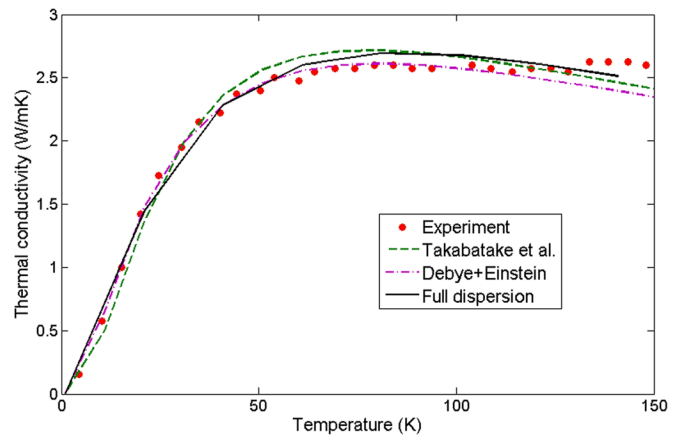


FIG. 5. Lattice thermal conductivity of  $\text{LaFe}_4\text{Sb}_{12}$  plotted versus temperature. Experimental data are taken from Takabatake *et al.*<sup>31</sup> Three models based on relaxation times approximation are used to fit the experimental data. The first two models are Debye + Einstein models which are using Debye dispersion and adding a resonance scattering term for Einstein frequencies. These two models are using different expressions for resonance scattering (Eq. (7) is used by Takabatake *et al.* and Eq. (8) is used for the plot labeled as Debye + Einstein). The third model is based on full dispersion. All fitting parameters for this plot are listed in Table I.

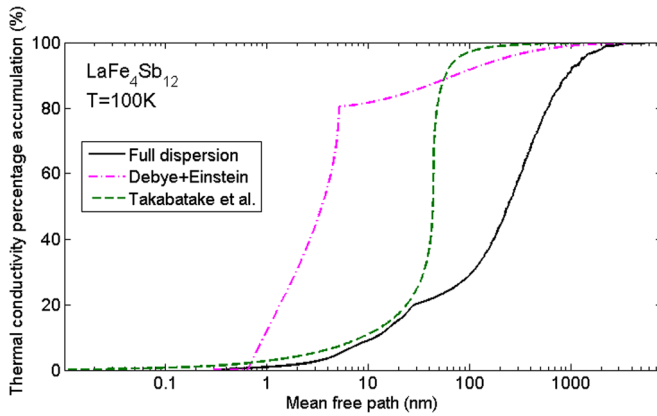


FIG. 6. Thermal conductivity percentage accumulation versus mean free path plotted at  $T = 100$  K for the three different models described in the text as well as in the caption of Fig. 5.

optical phonons are explicitly taken into account. The effect of filler atoms is to introduce extra optical bands and also to reduce the group velocity of the acoustic phonons.<sup>32</sup> According to Table I, phonon-phonon coupling is much stronger in the presence of the filler atoms, if we compare the  $B$  parameter reported from the full dispersion model for unfilled and fully filled skutterudites. However, if we look at the predictions by the Debye model, phonon-phonon coupling is weaker in the presence of the filler atoms and most of the reduction in the thermal conductivity is a result of resonance scattering. Using first-principles calculations, Feldman *et al.*<sup>33</sup> showed that there is a strong hybridization between bare La vibrations and certain Sb-like phonon branches, suggesting anharmonic scattering by harmonic motions of rare earth elements as an important mechanism for the suppression of the thermal conductivity. This is in agreement with the strong phonon-phonon scattering that we observed with the full dispersion model in fully filled  $\text{LaFe}_4\text{Sb}_{12}$ .

Figure 5 indicates that all three models can provide a good fit to the experimental data of the thermal conductivity. However, the values reported in Table I are very different from one model to the other. Therefore, there should be a large difference in the distribution of phonon mean free paths, as shown in Fig. 6, where the accumulative thermal conductivity versus mean free path is plotted for the three models. Note that in these fittings we tried to stay close to the fitting of Ref. 31.

Again the Debye based models underestimate the phonon mean free path inside fully filled skutterudites. According to these models, unless we reduce the grain size to values below 100 nm, there should be no difference between the measured lattice thermal conductivities. However, in the full dispersion model, phonons with a mean free path longer than 100 nm make more than a 70% contribution to the total thermal conductivity and as we reduce the grain sizes to values below  $1 \mu\text{m}$ , we should observe a large reduction in the lattice thermal conductivity.

Just like for the case of pure skutterudites, to confirm that nanostructuring is effective for  $\text{LaFe}_4\text{Sb}_{12}$ , we prepared samples of different grain sizes. High and low resolution SEM images are shown in Fig. 7 and the measured lattice

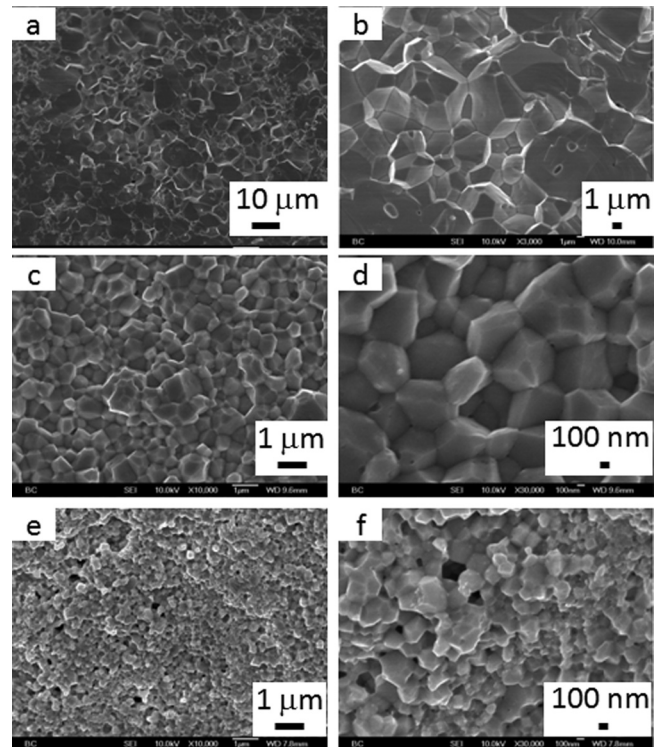


FIG. 7. Low- ((a)-(c) and (e)) and high- ((d) and (f)) magnification SEM images of the  $\text{LaFe}_4\text{Sb}_{12}$  samples with different grain sizes: S1: 2–10  $\mu\text{m}$  ((a) and (b)), S2: 0.5–1  $\mu\text{m}$  ((c) and (d)), S3: 200–500 nm ((e) and (f)).

thermal conductivities are reported in Fig. 8. If we look at the measured data at  $T = 100$  K, there is a clear difference in the measured thermal conductivities, despite the fact that the grain sizes are still larger than 100 nm for all samples. The only way to explain such a behavior is to rely on the predictions by full dispersions, not the Debye models. The predictions of the three models for samples of average grain size of

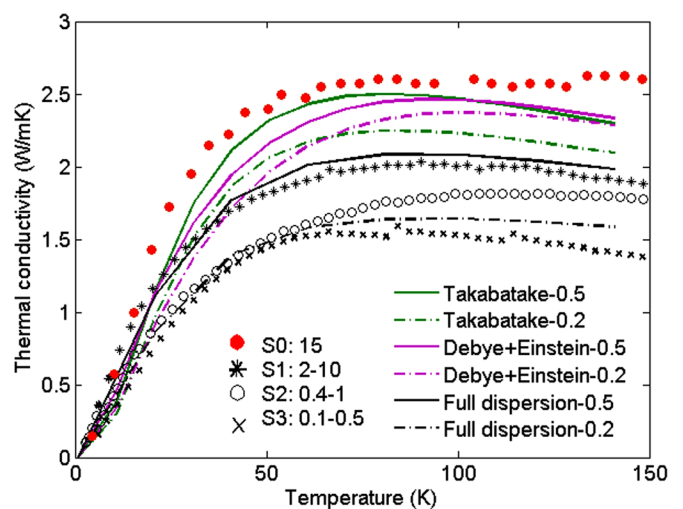


FIG. 8. Lattice thermal conductivity of  $\text{LaFe}_4\text{Sb}_{12}$  samples of different grain sizes. The data of sample S0 are taken from Takabatake *et al.*<sup>31</sup> Samples S1–S3 are prepared in our lab and their SEM images are shown in Fig. 7. The numbers in front of sample numbers indicate the grain size range in microns for each sample. We have fitted the bulk sample data (red dots) with three different models explained in the text and the fits are reported in Fig. 5. Here the predictions of the models for samples with average grain sizes of 0.5 and 0.2  $\mu\text{m}$  are reported.



500 nm and 200 nm are also shown in Fig. 8. Again it is not possible to directly compare the model with the experiment due to unknown size distribution of the grain sizes. However, clearly full dispersion predictions are closer to the experimental values of samples with similar grain sizes as those considered in the model.

## CONCLUSIONS

The thermal conductivity is an integrant over all phonon frequencies (only one number) and can be easily reproduced using simplified models with several fitting parameters. However, these simplified models do not necessarily result in correct distributions of the phonon mean free paths. Here, we showed that it is important to use the full dispersion and not the Debye model to get the correct mean free path spectrum. The Debye model underestimates the phonon mean free path both in the pure and fully filled skutterudites. Moreover, if we include resonance scattering combined with the Debye dispersion (Debye + Einstein model), the phonon-phonon scattering rate is underestimated. Experimental evidence shows that nanostructuring is an effective way to reduce the thermal conductivity of  $\text{Co}_4\text{Sb}_{12}$  in the temperature range of 300–600 K and also that of the  $\text{LaFe}_4\text{Sb}_{12}$  at low temperatures below 200 K, a result that is only consistent with the full dispersion predictions.

## ACKNOWLEDGMENTS

The study was supported by Bosch via the MIT Energy Initiative Program (G.C. and Z.F.R.). K. L., C.O., and M.S.D. are partially supported by the MIT S3TEC, an Energy Frontier Research Center funded by the U.S. Department of Energy, Office of Science; Office of Basic Energy Sciences under Award No. DE-FG02-09ER46577 for basic research in thermoelectric transport and materials and solar thermoelectric prototypes.

<sup>1</sup>A. F. Ioffe, *Thermoelements and Thermoelectric Cooling* (Infosearch Limited, London, 1957).

<sup>2</sup>G. Chen, *Phys. Rev. B* **57**, 14958 (1998).

<sup>3</sup>G. A. Slack and V. G. Tsoukala, *J. Appl. Phys.* **76**, 1665 (1994).

- <sup>4</sup>M. Zebarjadi, K. Esfarjani, M. S. Dresselhaus, Z. F. Ren, and G. Chen, *Energy Environ. Sci.* **5**, 5147–5162 (2012).
- <sup>5</sup>D. A. Broido, M. Malorny, G. Birner, N. Mingo, and D. A. Stewart, *Appl. Phys. Lett.* **91**, 231922 (2007).
- <sup>6</sup>A. Ward and D. A. Broido, *Phys. Rev. B* **81**, 085205 (2010).
- <sup>7</sup>J. Garg, N. Bonini, B. Kozinsky, and N. Marzari, *Phys. Rev. Lett.* **106**, 045901 (2011).
- <sup>8</sup>K. Esfarjani, G. Chen, and H. T. Stokes, *Phys. Rev. B* **84**, 085204 (2011).
- <sup>9</sup>J. Shiomi, K. Esfarjani, and G. Chen, *Phys. Rev. B* **84**, 104302 (2011).
- <sup>10</sup>G. Chen, *J. Heat Transfer* **119**, 220–229 (1997).
- <sup>11</sup>G. Chen and C. L. Tien, *ASME J. Heat Transfer* **114**, 636–643 (1992).
- <sup>12</sup>J. D. Chung, A. McGaughey, and M. Kaviani, *J. Heat Transfer* **126**, 376 (2004).
- <sup>13</sup>M. G. Holland, *Phys. Rev.* **132**, 2461 (1963).
- <sup>14</sup>D. Baillis and J. Randrianalisoa, *Int. J. Heat Mass Transfer* **52**, 2516 (2009).
- <sup>15</sup>N. Mingo, *Phys. Rev. B* **68**, 113308 (2003).
- <sup>16</sup>J. Callaway, *Phys. Rev.* **113**, 1046 (1959).
- <sup>17</sup>B. C. Sales, D. Mandrus, B. C. Chakoumakos, V. Keppens, and J. R. Thompson, *Phys. Rev. B* **56**, 15081 (1997).
- <sup>18</sup>J. L. Feldman and D. J. Singh, *Phys. Rev. B* **53**, 6273 (1996).
- <sup>19</sup>P. Ghosez and M. Veithen, *J. Phys.: Condens. Matter* **19**, 096002 (2007).
- <sup>20</sup>D. Wee, B. Kozinsky, N. Marzari, and M. Fornari, *Phys. Rev. B* **81**, 045204 (2010).
- <sup>21</sup>C. T. Walker and R. O. Pohl, *Phys. Rev.* **131**, 1433 (1963).
- <sup>22</sup>P. G. Klemens, in *Solid State Physics*, edited by F. Seitz and D. Turnbull (Academic, New York, 1958), Vol. 7, p. 1.
- <sup>23</sup>C. Dames and G. Chen, *Thermal Conductivity of Nanostructured Thermoelectric Materials CRC Handbook*, edited by M. Rowe (Taylor & Francis, Boca Raton, 2006).
- <sup>24</sup>B. C. Sales, D. Mandrus, B. C. Chakoumakos, V. Keppens, and J. R. Thompson, *Phys. Rev. B* **56**, 15081–15089 (1997).
- <sup>25</sup>D. Cao, F. Bridges, P. Chesler, S. Bushart, E. D. Bauer, M. B. Maple, *Phys. Rev. B* **70**, 094109 (2004).
- <sup>26</sup>V. Keppens, D. Mandrus, B. C. Sales, B. C. Chakoumakos, P. Dai, R. Coldea, M. B. Maple, D. A. Gajewski, E. J. Freeman, and S. Bennington, *Nature* **395**, 876–878 (1998).
- <sup>27</sup>N. R. Dilley, E. D. Bauer, M. B. Maple, S. Dordevic, D. N. Basov, F. Freiberger, T. W. Darling, A. Migliori, B. C. Chakoumakos, and B. C. Sales, *Phys. Rev. B* **61**, 4608 (2000).
- <sup>28</sup>B. C. Sales, B. C. Chakoumakos, and D. Mandrus, *Mater. Res. Soc. Symp.* **626**, 2000.
- <sup>29</sup>R. P. Hermann, F. Grandjean, and G. J. Long, *Am. J. Phys.* **73**, 110 (2005).
- <sup>30</sup>G. S. Nolas, T. J. R. Weakley, J. L. Cohn, and R. Sharma, *Phys. Rev. B* **61**, 3845 (2000).
- <sup>31</sup>T. Takabatake, E. Matsuoka, S. Narazu, K. Hayashi, S. Morimoto, T. Sasaki, K. Umeo, and M. Sera, *Physica B* **383**, 93–102 (2006).
- <sup>32</sup>M. Zebarjadi, K. Esfarjani, J. Yang, Z. F. Ren, and G. Chen, *Phys. Rev. B* **82**, 195207 (2010).
- <sup>33</sup>J. L. Feldman, D. J. Singh, I. I. Mazin, D. Mandrus, and B. C. Sales, *Phys. Rev. B* **61**, R9209–R9212 (2000).